SYNAPSE 56:154–165 (2005)

Electrical Synapse Formation Disrupts Calcium-Dependent Exocytosis, But Not Vesicle Mobilization

JOSHUA P. NEUNUEBEL AND MARK J. ZORAN*
Department of Biology, Texas A&M University, College Station, Texas 77843

KEY WORDS gap junction; neurotransmission; synaptogenesis; presynaptic mechanisms

ABSTRACT Electrical coupling exists prior to the onset of chemical connectivity at many developing and regenerating synapses. At cholinergic synapses in vitro, trophic factors facilitated the formation of electrical synapses and interfered with functional neurotransmitter release in response to photolytic elevations of intracellular calcium. In contrast, neurons lacking trophic factor induction and electrical coupling possessed flash-evoked transmitter release. Changes in cytosolic calcium and postsynaptic responsiveness to acetylcholine were not affected by electrical coupling. These data indicate that transient electrical synapse formation delayed chemical synaptic transmission by imposing a functional block between the accumulation of presynaptic calcium and synchronized, vesicular release. Despite the inability to release neurotransmitter, neurons that had possessed strong electrical coupling recruited secretory vesicles to sites of synaptic contact. These results suggest that the mechanism by which neurotransmission is disrupted during electrical synapse formation is downstream of both calcium influx and synaptic vesicle mobilization. Therefore, electrical synaptogenesis may inhibit synaptic vesicles from acquiring a readily releasable state. We hypothesize that gap junctions might negatively interact with exocytotic processes, thereby diminishing chemical neurotransmission. **Synapse 56:154–165, 2005.**

INTRODUCTION

Electrical coupling, mediated by gap junctions, exists transiently between neurons and targets in both developing and regenerating nervous systems. These electrical synapses constitute a temporary mechanism of cellular communication, permitting the passage of ions and small molecules through junctional pores into neighboring cells (Veenstra et al., 1995; Nicholson and Bruzzone, 1997; Bennett and Zukin, 2004). Electrotonically coupled cells are present in the development of the spinal cord; for example, *Xenopus* neurons maintain electrical connectivity until Na^+-based action potentials emerge (Spitzer, 1982). The developing mammalian neocortex transiently expresses gap junctions that have been implicated in coordinating the mitotic phases in groups of clonally related cells (Bittman et al., 1997; reviewed in Sutor, 2002). In the developing vertebrate visual system, both ions and second messengers pass through gap junctions, potentially resulting in synchronous biochemical activity (Kandler and Katz, 1998). In addition to embryonic development, transient electrical synapses exist following axotomy of mammalian PNS neurons, which suggests a role in regeneration (Chang et al., 2000). Despite appearing in both developing and regenerating nervous systems, the role of these short-lived intercellular connections remains elusive.

Since transient electrical synapses occurs at many developing synapses prior to the onset of chemical neurotransmission, a role for gap junctional coupling in the synaptogenic establishment of functional neural networks has been suggested (reviewed in Kandler and Katz, 1995). A temporal pattern of electrical communication preceding chemical connectivity

Contract grant sponsor: NINDS; Contract grant number: PO1 NS-39546 (to M.J.Z.).

*Correspondence to: Dr. Mark J. Zoran, Department of Biology, Texas A&M University, College Station, TX 77843. E-mail: zoran@mail.bio.tamu.edu

Received 6 August 2004; Accepted 12 January 2005

DOI 10.1002/syn.20139

Published online in Wiley InterScience (www.interscience.wiley.com).

exists during the development of frog neuromuscular junctions (Allen and Warner, 1991), both vertebrate and invertebrate visual systems (Curtin et al., 2002; Penn et al., 1994), and mouse motor neurons (Personius et al., 2001). Chemical neurotransmission is inhibited in neonatal rats, when gap junctional coupling increases (Mentis et al., 2002; Pastor et al., 2003). Furthermore, trophic factor-dependent expression of electrical connectivity delays the onset of functional chemical neurotransmission at regenerating synapses in *Helisoma* (Szabo et al., 2004).

Helisoma motor neurons B19 and B110, in cell culture, exhibit transient electrical connections that are maintained for several days. Intercellular coupling is subsequently replaced by inhibitory chemical synaptic transmission at these synapses and the acquisition of functional neurotransmission is dependent on the suppression of gap junctional communication (Szabo et al., 2004). This inverse relationship between electrical and chemical transmission is virtually identical to the pattern of synaptogenesis observed between these neurons following axotomy in vivo and suggests that electrical synaptic mechanisms facilitate the exclusion of functional chemical neurotransmission at developing synapses. Since the nature of both electrical and chemical synapse formation has been extensively examined in *Helisoma* neurons (Bulloch and Kater, 1981; Bulloch et al., 1980; Hadley et al., 1982, 1983, 1985; Haydon and Kater, 1988; Zoran et al., 1996) and giant somatic synapses allow for precise spatial and temporal resolution of synaptic properties (Haydon and Zoran, 1989; Hamakawa et al., 1999; Szabo et al., 2004), we used this system to test the hypothesis that electrical synapse formation mediates the functional exclusion of chemical neurotransmission at synaptic contacts formed between *Helisoma* neurons 110 and 19 in cell culture. In the present studies, we examined the potential role of electrotonic/biochemical coupling in 1) the regulation of voltage-dependent calcium accumulation, 2) the shunting of presynaptic calcium by cell to cell diffusion, 3) the regulation of postsynaptic receptor sensitivity, and 4) the developmental mobilization of the presynaptic secretory vesicles. Our data suggest that transient electrical coupling does not disrupt these fundamental mechanisms of chemical neurotransmission and that the process of electrical synapse formation (or the trophic mechanism that induces it) mediates a functional block between the accumulation of presynaptic calcium and synchronized, vesicular release of neurotransmitter.

MATERIALS AND METHODS

Animals

Laboratory stocks of American pond snails, *Helisoma trivolvis*, were cultured in 20-gallon aquaria at 22°C. Snail cultures were maintained on a 12/12-h light/dark photoperiod and fed daily on a combination of trout chow and lettuce.

Cell culture

Two motor neurons, B110 and B19, were isolated from buccal ganglia based on location, pigmentation, and morphology as previously described (Zoran et al., 1991; Poyer and Zoran, 1996). Cells were placed in conditioned medium (CM) for 3 days, which allowed for absorption of original axons and the formation of spherical somata. CM was prepared by incubating two ring-ganglia per 1 mL of defined medium (DM) in sigma-coated (Sigma, St. Louis, MO) glass culture dishes. After 3 days, neurons were paired and transferred to 35-mm plastic culture dishes (No. 1008 Falcon, Oxnard, CA) containing 2 mL of either CM or DM medium for 24 h. The plastic culture dishes were made nonadhesive through pretreatment with a 0.5% solution of bovine serum albumin (BSA).

Electrophysiology

Electrophysiological experiments were conducted using intracellular, current-clamp techniques. Preparations were viewed and imaged with an Olympus IX70 inverted microscope. Dual glass electrodes (Borosil 1.5 mm, FHC), filled with 1.5 M KCl (10–20 MΩ), were used for simultaneous recordings (pre- and postsynaptic) of neuronal pairs. Cell pairs were plated on poly-L-lysine (Sigma)-coated culture dishes (plastic or coverglass bottom) containing DM. The neuronal membrane potential was held at approximately –75 mV before base current injection. Electrical synapses were detected by injecting a hyperpolarizing current step using a Grass S48 stimulator and bridge-balanced electrometers (Model 5A, Getting Instruments, San Diego, CA). Electrophysiological input signals were converted from analog to digital by MacLab software (AD Instruments, Charlotte, NC) and a Macintosh computer. The digitized data were archived and later analyzed with MacLab Chart software. Electrical coupling was calculated using the following formula (see Szabo et al., 2004): ECC = (Δ Vm postsynaptic cell) / (Δ Vm presynaptic cell).

Digital microscopy

Neurons were viewed at 40× magnification for differential interference contrast microscopy (DIC; objective, NA = 0.6) or ratiometric calcium imaging (Fura-2 oil objective, NA = 0.65). For Fura-2 experiments, excitation light was emitted from a computer-controlled Lambda DG4 monochromator (Sutter Instrument, Novato, CA). The excitation light path included passage through 1.0 or 1.3 neutral density transmission filters and the excitation filters (340 and 380 nm).

A dichroic mirror (400 nm) and emission filter (510 nm) were used for collection of emitted fluorescence. A digital CCD camera (OreaER; Hamamatsu, Bridgewater, NJ) collected 2 × 2 binning images at variable exposures.

Intracellular pressure injections

Sharp glass pipettes, with a tip diameter ranging from 0.5–1.0 μm, were created from capillary tubes (Borosil 1.5 mm, FHC) and filled with internal solutions of either fluorescent calcium indicators or NP-EGTA preloaded with calcium. Solutions were pressure-injected with a Picospritzer II (General Valve, Marietta, GA). The duration of the injection pulses was 5–10 msec at 20–30 psi. Solutions were injected until the diameter of the cell detectably increased by ~5–10%. Therefore, the final cytosolic concentrations were lower than that contained in the pipette.

Calcium imaging

Cells were loaded for 1 h with the cell permeable calcium-sensitive probe Fura-2 AM (Molecular Probes, Eugene, OR) at a final concentration of 5 μM in DM, or pressure-injected (as previously described) with Fura-2, pentapotassium salt (Molecular Probes). The membrane-permeable calcium dye was washed from the cells by transferring them through two 30-min DM baths. After washing, the cells were plated on poly-L-lysine-coated coverglass slides. Cell pairs injected with the cell impermeable version of Fura-2 were plated prior to loading.

Fura-2 fluorescence was viewed in the manner indicated earlier. SimplePCI software (Compix) was used to determine F_{340}/F_{380} ratios for intracellular calcium concentrations from image pairs collected at rates of 2–4 pairs/sec. A portion of the image devoid of cells, processes, or debris was sampled for background subtraction. Calcium concentrations were calculated using the ratio of Fura-2 excitation at 340 and 380 (Grynkiewicz et al., 1985) with the equation: $[Ca^{2+}] = K_d \times [R - R_{min}/R_{max} - R] \times (F_{max380}/F_{min380})$. $[Ca^{2+}]$ represents the intracellular free calcium concentration, K_d is the dissociation constant of calcium from the dye (224 nM), and R is the calculated ratio intensity. Zero and saturation calcium intensity ratios are denoted by R_{min} (0.251) and R_{max} (10.876), respectively. F_{max380} (210.8) is the fluorescence intensity measured at zero calcium, and F_{min380} (18.9) is the fluorescence intensity measured when the cells were saturated. These values were determined for this imaging system using cell-free methods and Fura-2 calibration standards (Molecular Probes).

Calcium manipulation

Flash photolysis of ω-nitrophenyl EGTA (NP-EGTA, Molecular Probes), preloaded with calcium, was implemented to experimentally manipulate intracellular calcium concentrations. Presynaptic neurons were pressure-injected (as previously described) with a solution that contained 40 mM NP-EGTA, 32 mM $CaCl_2$, and 10 mM Hepes at pH 7.4. Neurons were allowed to recuperate from the injection for 15–30 min. After obtaining resting calcium levels for 10 sec (as formerly mentioned), electronically controlled shutters (Prior) were opened for 2–3 sec, exposing cells to UV light emitted from an Olympus mercury vapor lamp. Ratiometric image pairs were captured before and after UV exposure for calcium estimations.

UV-evoked neurotransmitter release

Neurotransmitter release was estimated by calculating the total area under the postsynaptic potential (PSP) trace following UV photolysis of NP-EGTA. Area under the PSP curve was determined by analyzing images of postsynaptic electrophysiological recordings (Adobe PhotoShop 6, San Jose, CA). A contiguous line was extended that connected the extrapolated baseline (resting potential) to the depolarizing postsynaptic membrane potentials. Image J (NIH Image) software was used to calculate the total area in pixels encompassed by this line. A relative neurotransmitter release index was determined for both CM and DM preparations, where an index of 1 equals 1,000 pixels of area under a PSP curve.

Postsynaptic receptor sensitivity

Neuronal pairs were cultured in CM or DM for 24 h and then transferred to a poly-L-lysine-coated 1008 culture dish containing DM. ACh (10 μM; Sigma), contained in a glass pipette (~1 μm tip) positioned 5–10 μm from the postsynaptic cell membrane, was focally applied to the B19 with 5-msec pulses provided by a Picospritzer II (30 psi). Tubocurarine chloride (3.75–10 μM; Sigma) antagonized the effects of ACh at these synapses.

Synaptic vesicle imaging

Synaptic vesicles were stained with FM 1-43 (Molecular Probes) to monitor vesicle recruitment during synapse formation. Prior to cell contact, nascent presynaptic neurons (B110s) were incubated for 5 min in a solution of high potassium DM (50 mM KCl) and 2.5 μM FM 1-43. Negative control cells were depolarized in high K^+ DM that lacked the synaptic vesicle stain. Following the depolarization-facilitated loading the cells were washed in DM. The loading and wash procedure was repeated two additional times to ensure pervasive vesicle staining. B110s were cul-

tured, either isolated or with B19s, in the appropriate medium for 24 h. After plating on coverglass dishes containing DM, fluorescence images were acquired using rhodamine optics (excitation: 530–550 nm; dichroic mirror: 570 nm; emission: 590 nm) and digital photography. Fluorescence intensity was determined for individual neurons. Regions of interest (ROIs) were digitally selected and the background intensity was subtracted. An arbitrary point on a single cell was chosen for the first ROI (7 μm in diameter). Subsequently, every 30° (clockwise and counterclockwise) an additional ROI was analyzed. Two groups, each containing three ROIs—one proximal and one distal to the synapse—were chosen to represent synaptic vesicle distribution in neuronal pairs.

Data analysis

SPSS software (SPSS, Chicago, IL) was used to analyze experimental datasets. Mann-Whitney or Wilcoxon Signed tests were implemented for data analysis as indicated in the text. Values are displayed as the mean plus or minus the standard error of the mean (SEM). Statistical significance was defined as $P < 0.05$.

RESULTS

Giant somatic synapses, derived from the nervous system of *Helisoma*, exhibited differences in intercellular coupling when cultured with and without exposure to trophic factors in conditioned medium (Fig. 1). An electrical coupling coefficient (ECC) of 0.34 ± 0.05 was calculated for cell pairs cultured in CM, medium containing trophic factors. In contrast, pairs incubated in DM, medium lacking trophic factors, possessed an ECC of 0.14 ± 0.05. These ECC values for CM and DM groups were significantly different ($P < 0.002$; n = 18 per group; Fig. 1C). In six cell pairs from each group, the presynaptic B110 was injected with the photolytic calcium cage, NP-EGTA, and then exposed to a brief UV light flash to elevate presynaptic calcium levels (Fig. 2A). An inverse relationship between electrical synapses and chemical neurotransmission was obvious in these cell pairs (Fig. 2B–E). Synapses with strong electrical coupling (i.e., CM pairs; Fig. 2B) did not respond to photolytic elevation in calcium with release of neurotransmitter (Fig. 2C). At synapses that lacked detectable electrotonic transmission (i.e., DM pairs; Fig. 2D), large PSPs were induced by UV flash (Fig. 2E). Photolytic release of calcium-induced postsynaptic potentials (PSPs) of significantly greater magnitude at DM-cultured synapses than at CM-cultured synapses ($P < 0.02$; Fig. 2F). Since the initial photolytic flash resulted in partial depletion of caged calcium, subsequent photolysis resulted in decreased calcium release and, as a result, reduced the size of the PSP (Fig. 2E,F). UV-photolysis of the caged calcium did not generate changes in presynaptic membrane potential or, in CM pairs, changes in postsynaptic potential (Fig. 2C).

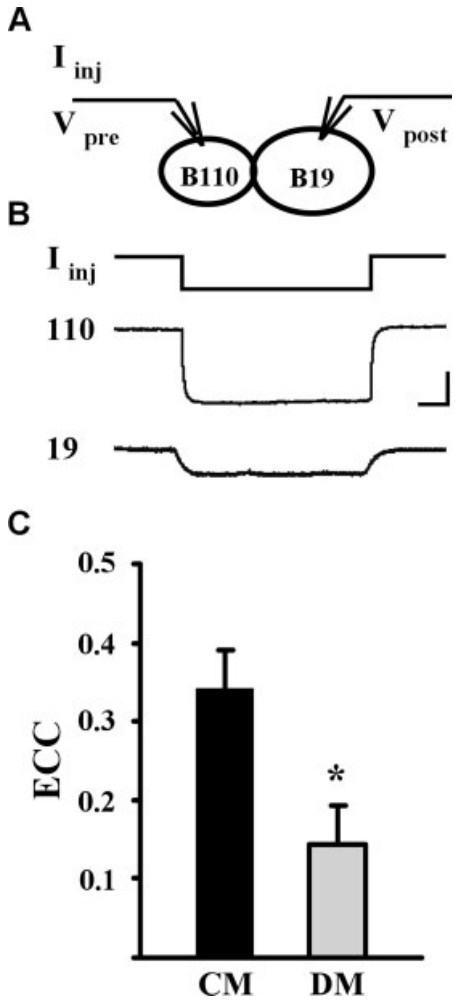

Fig. 1. Trophic factors promote electrical synapse formation. **A:** Electrophysiological recording configuration for manipulation and assessment of presynaptic and postsynaptic membrane potentials. Hyperpolarizing current (I_{inj}) was injected into the presynaptic neuron B110 for the purpose of monitoring electrical coupling. **B:** Representative recordings of electrical coupling in B110-B19 cell pairs cultured in CM. The onset and termination of the current injection pulse is indicated in the top trace. Membrane potentials were current-clamped for both neurons B110 (middle trace) and B19 (bottom trace) at approximately –75 mV prior to the hyperpolarizing current injection. Horizontal bar = 1.0 sec; vertical bar = 20 mV. **C:** CM cell pairs (n = 18; black bar) exhibited a strong electrical coupling coefficient (ECC) whereas DM pairs (n = 18; gray bar) were significantly less coupled (*$P < 0.002$). Data represent mean ± SEM.

To determine if photolytic release of caged-calcium effectively elevated intracellular calcium concentrations in both CM and DM groups, we monitored presynaptic calcium using the ratiometric fluorescent indicator, Fura-2 AM (Fig. 3A–D). In neuronal pairs cultured in CM, an average resting calcium concentration of 150 ± 25 nM was elevated to 460 ± 100 nM

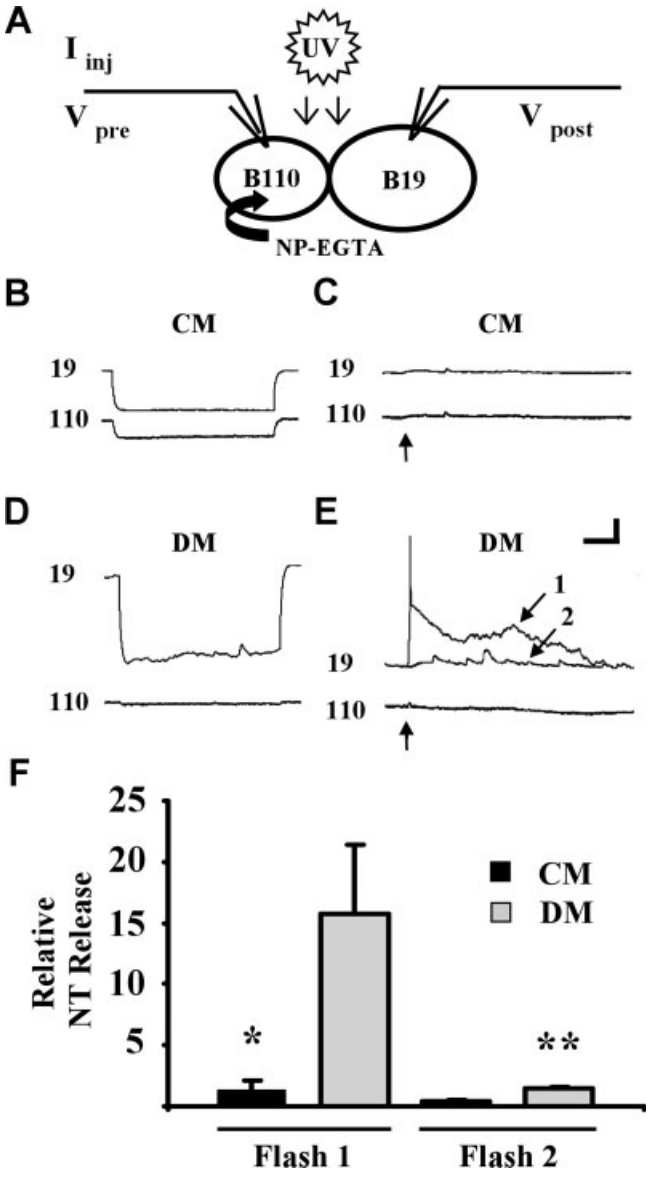

Fig. 2. Photolytic release of calcium-induced neurotransmitter secretion at uncoupled, but not electrically coupled, synapses. **A:** Arrangement for intracellular recordings and NP-EGTA loading (black arrow) in cell pairs. **B–E:** An inverse relationship existed between electrotonic coupling and NP-EGTA/UV-evoked neurotransmitter release. Electrophysiological recordings of electrical coupling in cell pairs cultured in CM (**B,C**) and DM (**D,E**) are paired with respective recordings of neurotransmitter release in these same cell pairs. Membrane potential recordings of neuron B19 (top) and B110 (bottom) are shown. Horizontal bar = 1.0 sec; vertical bar = 20 mV. **C:** Following UV pulse (arrow), no change was detected in membrane potential in either neuron of this CM pair. **E:** In a DM cell pair, the first UV pulse (trace #1) generated a significant change in the membrane potential of B19 (postsynaptic cell). A second UV pulse (trace #2) elicited a significantly smaller postsynaptic response. There was no change in membrane potential of B110 (presynaptic cell). **F:** Quantification of the levels of chemical neurotransmission as measured by relative magnitude of PSPs. Following the first UV pulse, CM cell pairs (n = 7) exhibited significantly less neurotransmission than DM pairs (*$P < 0.02$). After a second UV pulse, secretion was significantly reduced in DM pairs (**$P < 0.01$).

following UV photolysis (Fig. 3F). Similarly, the average resting calcium level in DM pairs was 100 ± 15 nM and after photolysis increased to 480 ± 95 nM. Subsequent flashes of UV light caused reduced calcium transients as the NP-EGTA cage was depleted of calcium (Fig. 3E). Although photolysis resulted in a significant increase in presynaptic calcium in both CM (n = 9; $P < 0.01$) and DM pairs (n = 8; $P < 0.02$), there was no difference in the final level of calcium attained between the two groups (Fig. 3F). Furthermore, B110 presynaptic neurons, in both CM and DM groups, attained similar levels of intracellular calcium following electrical stimulation (current injection) and subsequent membrane depolarization (data not shown; CM = 313 ± 68 nM; DM = 348 ± 113 nM; $P = 0.99$). Therefore, the ability of DM synapses, but not CM synapses, to respond to photolysis with calcium-dependent exocytosis was not due to differential function of NP-EGTA in the two trophic environments. Additionally, synapses formed in these disparate culture conditions did not differ in their capacities to buffer changes in intracellular calcium.

To determine if the presence of electrical synapses or trophic stimulation altered postsynaptic receptor sensitivity, and thereby chemical neurotransmission, we examined postsynaptic neuronal responses to acetylcholine (ACh) using a combination of electrophysiological and pharmacological techniques (Fig. 4A). The average ECC in CM pairs (n = 11) was 0.27 ± 0.06 compared to 0.06 ± 0.03 in DM pairs (n = 12) in this experiment. Following focal application of ACh to the postsynaptic cell of the giant synapse, both CM and DM preparations displayed an increase in postsynaptic membrane voltage (Fig. 4B). No significant difference in postsynaptic membrane potential change was found between CM and DM groups (Fig. 4C). One minute after applying 3.75 μM tubocurarine chloride (curare, a cholinergic receptor antagonist), ACh-evoked responses were abolished in both CM and DM pairs (data not shown). Thus, differences in sensitivity to ACh between DM and CM cultured synapses were not detectable in this study.

Since calcium-dependent regulation of neurotransmitter release is a process localized to sites of vesicle fusion at the presynaptic membrane, we hypothesized that gap junctional coupling at these synapses might form a conduit to shunt calcium. For this to occur, calcium ions would move down their concentration gradient into the postsynaptic cell during an action potential, or photolytically induced, presynaptic elevations. To test this, we monitored postsynaptic calcium levels at giant somatic synapses using Fura-2 (Fig. 5A–D). After UV photolysis of NP-EGTA in the presynaptic neuron, no significant difference was detected between the postsynaptic calcium concentrations in CM and DM pairs ($P = 0.67$; Fig. 5E). Furthermore, in CM-cultured synapses that possessed

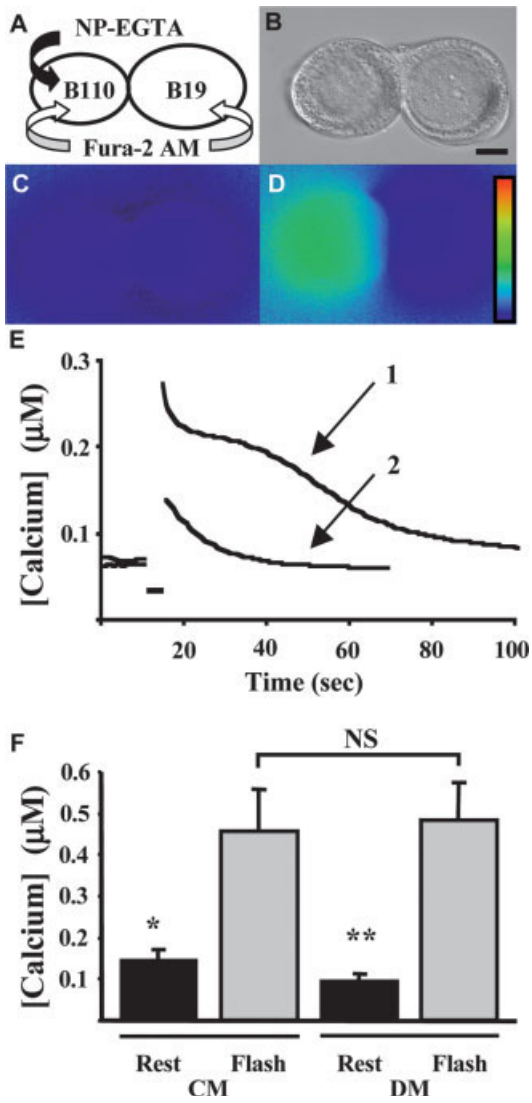

Fig. 3. NP-EGTA photolysis elevated presynaptic calcium levels equally in CM and DM cultured somatic synapses. **A:** Illustration of the loading procedure utilized to manipulate (Ca^{2+}-loaded NP-EGTA; closed arrow) and visualize (Fura-2; open arrow) intracellular calcium. **B:** The Nomarski image of the giant somatic synapse shows a typical B110-B19 neuronal pair cultured in DM (B110 is on the left). Scale bar = 10 μm. **C,D:** The representative fluorescent images indicate resting calcium levels before UV photolysis (**C**) and the elevated calcium concentration in B110 after photolysis (**D**). On the scale bar, the transitions between blue-green and green-orange are ~100 nM and 1,000 nM, respectively. **E:** Calcium concentration for a DM pair after an initial (arrow 1) and a subsequent (arrow 2) flash of UV light. The first pulse elevated the calcium concentration to at least 300 nM, which was twice the level generated from the second pulse. Bar indicates period of no calcium data collection during UV illumination. **F:** The graph represents the average intracellular calcium concentration in B110 for both CM and DM cell pairs. There was a significant rise in presynaptic calcium concentration after UV photolysis for both CM (n = 9) and DM (n = 8) controls (*$P < 0.01$; **$P < 0.02$); however, there was no significant difference in the intracellular calcium concentration between the presynaptic neurons in CM and DM before (rest; $P = 0.2$) or after photolysis (flash; $P = 0.81$).

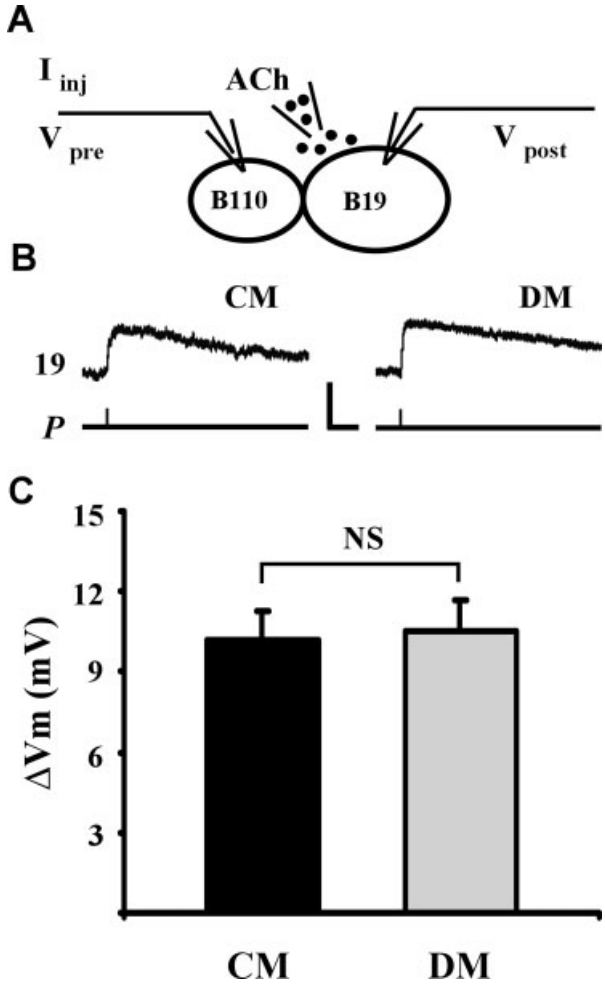

Fig. 4

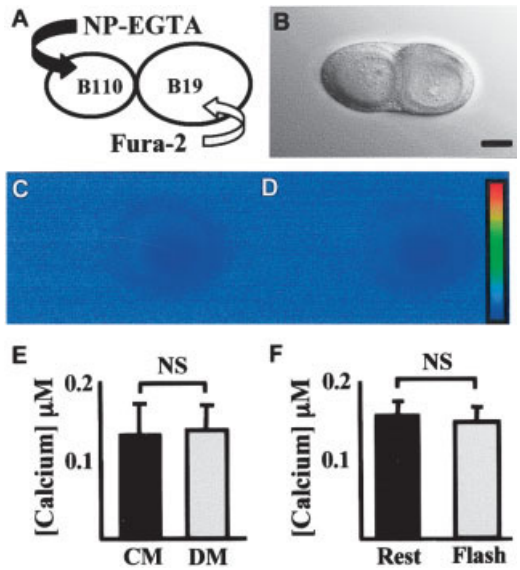

Fig. 5

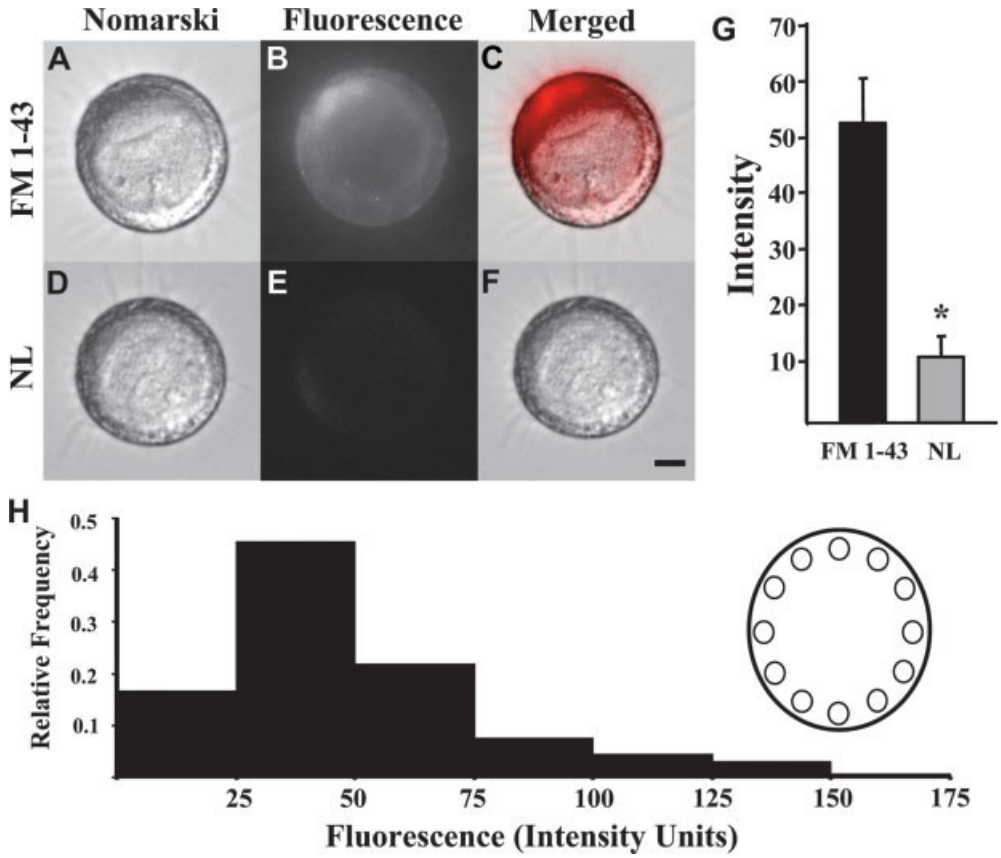

Fig. 6. Isolated presynaptic neurons possessed hotspots of vesicle clustering, as indicated by FM 1-43 staining. **A–F:** Images of single cells stained with FM 1-43 following high K^+ stimulation loading (FM 1-43; **A–C**) and nonloaded (NL; **D–F**) cells stimulated in the absence of dye. Images were acquired using Nomarski (**A,D**) or fluorescence (**B,E**) optics and then merged (**C,F**). Scale bar = 10 μm. In single cell loading, the entire cell contained synaptic vesicles stained with FM 1-43; however, some areas of the cytoplasm exhibited greater uptake of dye (upper left of cytosol in **B,C**). **G:** Fluorescence intensity of a neuron exposed to FM 1-43 (FM 1-43; n = 11) was significantly greater than control intensity (NL; n = 5; $*P < 0.003$). **H:** Distribution of fluorescence intensity, as described by selected ROIs. Twelve ROIs (7 μm in diameter each) spaced 30° apart were chosen around the neuronal perimeter (schematic inset). 67% of the ROIs possessed intensities ranging from 26–75, with an overall range of 1–175. All cells possessed "hotspots" with greater fluorescence intensities.

Fig. 4. Suppression of chemical neurotransmission at electrically coupled synapses was not due to changes in postsynaptic cholinergic receptor sensitivity. **A:** Experimental configuration employed to test for the presence of functional postsynaptic cholinergic receptors. After determining the ECC at a synapse, ACh was focally applied to the postsynaptic membrane to examine postsynaptic sensitivity. **B:** Representative recordings of ACh-evoked potentials in CM or DM cultured cell pairs showed similar changes in amplitude. The time lines, running below the traces, indicate the moment (5 ms pulse (*P*)) when ACh was administered. Horizontal scale bar = 1 sec; vertical scale bar = 5 mV. **C:** Average peak PSP amplitudes following ACh application were not significantly different between CM (n = 12) and DM (n = 13) pairs ($P = 0.7$).

Fig. 5. Experimental elevation of presynaptic calcium did not alter postsynaptic calcium levels. **A:** Conformation employed for manipulation of intracellular presynaptic calcium (Ca^{2+} loaded NP-EGTA; closed arrow), and detection of postsynaptic calcium levels (Fura-2; open arrow). **B:** Representative DIC/Nomarski image showing a giant somatic synapse cultured in CM. Scale bar = 10 μm. **C,D:** These representative fluorescence images indicate the calcium levels in B19 before and after UV photolysis for this cell pair. No change in postsynaptic calcium was detected. On the scale bar, transitions between blue-green and green-orange are ~100 nM and 1,000 nM, respectively. **E:** Average postsynaptic calcium concentration between CM (n = 13) and DM (n = 5) cell pairs after UV photolysis were not significantly different ($*P = 0.67$). **F:** In electrically coupled CM cell pairs (n = 3; ECC = 0.34), no significant difference in postsynaptic calcium concentration was observed when comparing levels before (rest) and after UV photolysis (flash; $*P = 0.11$).

the strongest electrical coupling (i.e., average ECC of 0.35 ± 0.15; n = 3), no change in postsynaptic calcium concentrations were detected following photolysis (Fig. 5F). Thus, no evidence of calcium movement from presynaptic to postsynaptic neurons emerged from these studies.

Having determined that differences in presynaptic calcium elevations and postsynaptic sensitivity were not detectable between CM and DM cell pairs, we examined the nature of synaptic vesicle mobilization at these synapses. We tested the hypothesis that electrically coupled synapses formed in CM possess a diminished capacity for secretory machinery recruitment, thereby impeding functional neurotransmission. To address this idea, the fluorescent vesicle dye, FM 1-43, was used to stain synaptic vesicles in isolated B110 neuronal somata (i.e., only the "presynaptic" neurons) prior to contact with the target cell. Following a stimulation/dye-loading protocol (see Materials and Methods), there was a significant increase in fluorescence intensity (i.e., staining) of

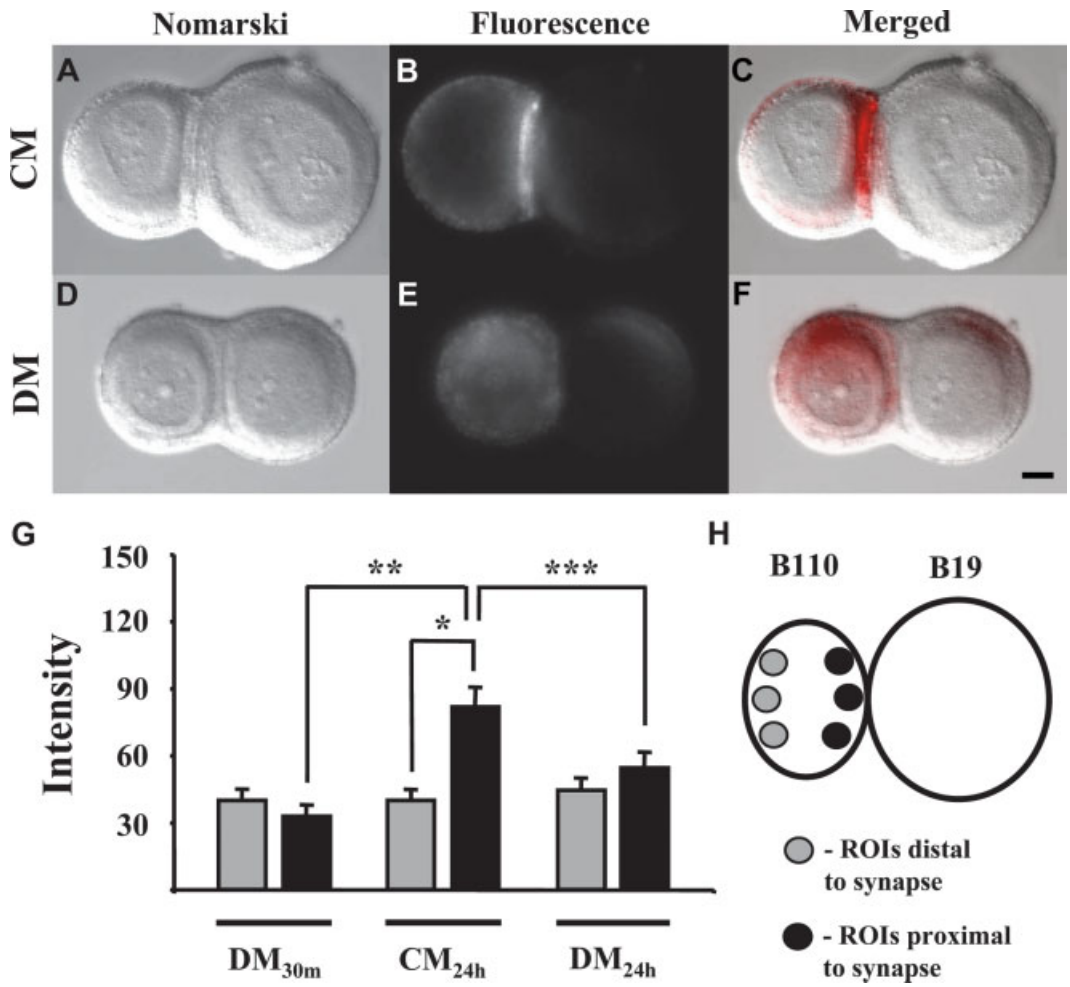

Fig. 7. Trophic factors enhanced vesicle mobilization in the absence of chemical neurotransmission. **A–F:** Representative images of cell pairs cultured for 24 h in either CM or DM. Images were acquired using Nomarski (**A,D**) or fluorescence (**B,E**) optics and then merged (**C,F**). Panels **A, B, C, G** illustrate cell pairs cultured in CM for 24 h and reveal the presence of stained synaptic vesicles around the peripheral cytoplasm; however, a heavy band of staining is visible at the newly forming synapse. **D–G:** Neuronal pairs cultured in DM for 24 h exhibit no significant accumulation of staining at the synapses, but more of a comprehensive distribution. Scale bar = 10 μm. **G,H:** Fluorescence intensity in CM-cultured cell pairs possessing strong electrical coupling was significantly greater than in DM-cultured pairs at sites of synaptic contact. Three ROIs proximal (black) and three distal (gray) to the synapse were examined following contact for 30 min in DM (DM_{30m}; n = 7), 24 h in CM (CM_{24h}; n = 15), or 24 h in DM (DM_{24h}; n = 14). FM 1-43 fluorescence intensity near the synapse was significantly greater in CM than in either DM group (**$P < 0.002$; ***$P < 0.04$). Differences between groups at distal ROIs were not observed. Within the group of CM-cultured neuronal pairs, greater fluorescence was observed at ROIs proximal vs. distal to the synapse (*$P < 0.003$).

these individual neurons compared to controls (stimulated without dye; $P < 0.003$; Fig. 6A–G). Although dye was incorporated into these isolated neurons, cells were not uniformly loaded; that is, some regions of the cytoplasm contained greater fluorescence intensity, suggesting a higher level of vesicle turnover at "hotspots" prior to the commencement of synaptogenesis. An analysis of 12 ROIs (see Materials and Methods) around the periphery of stained B110 neurons revealed that hotspots constituted ~10% of all ROIs prior to the formation of synaptic contact (Fig. 6H).

Synaptic vesicles, imaged by FM1-43 staining, were localized to sites of contact at newly forming synapses possessing electrical coupling (Fig. 7). ROIs for FM1-43 analysis were selected at consistent locations among presynaptic cells (see Fig. 7H for ROI locations). One ROI was chosen at the center point of the synapse and two additional sites were chosen at positions 30° clockwise and counterclockwise. A complementary set of three ROIs was selected on the opposite side of the presynaptic neuron (i.e., away from the site of cell–cell contact). The three ROIs at the site of contact in CM pairs, following 24 h of synapse formation, possessed high fluorescent intensity as compared to three ROIs distal to the site of synaptic contact (Fig. 7A–H). Fluorescence was more homogeneously distributed in DM pairs (Fig. 7A–H). Pronounced bands of fluorescent staining were present at the interface (sites of cell–cell contact) between neuronal pairs in CM culture, but not DM culture

(Fig. 7B,C). Fluorescent intensity was not significantly greater at presynaptic sites of cell–cell contact after 24 h in DM as compared to cells after only 30 min of contact ($P = 0.052$; Fig. 7G). When comparing synaptic vesicle distribution for each of the three groups, only neuronal pairs cultured in CM exhibited a significant increase in fluorescence at ROIs proximal to the synapse compared to the most distal regions ($P < 0.003$; Fig. 7G). Thus, mobilization of synaptic vesicles occurred at CM-cultured synapses. These studies demonstrated that a mechanism associated with electrical synapse formation (electrical coupling, biochemical coupling, and/or gap junction-mediated signaling processes) in CM-cultured neuronal pairs enhanced vesicle recruitment and possibly facilitated the chemical synaptogenic process.

DISCUSSION

The establishment of physical contact between neurons, in many embryonic and regenerating nervous systems, triggers a developmental progression of synaptic communication involving an initial formation of electrical connectivity that switches to predominantly chemical neurotransmission as electrotonic coupling declines (Allen and Warner, 1991; Penn et al., 1994; Personius et al., 2001; Chang et al., 2000; Szabo et al., 2004). These observations prompt the speculation that gap junctional intercellular communication coordinates electrical or biochemical neuronal activities during initial phases of synaptogenesis (Kandler and Katz, 1995). Strength of electrical coupling is inversely correlated with the amplitude of chemically transmitted synaptic potentials during early synaptogenesis between cultured *Helisoma* neurons (Szabo et al., 2004). This observation indicates that the presence of gap junctional coupling delays the onset of chemical neurotransmission by means of a mechanistic interaction between the two forms of synaptic communication. Here, we investigated the mechanism by which electrical coupling might delay chemical connectivity at developing synapses and demonstrated that cell culture conditions that promote electrical synapse formation also suppress transmitter release by disrupting the capacity for a presynaptic calcium influx to trigger vesicular exocytosis. Therefore, we hypothesize that electrical synapses provide a developmental mechanism for modulating the emergence of chemical neurotransmission at newly forming synaptic contacts, thereby potentially influencing the establishment of neural networks.

Exposure of giant somatic synapses to ganglia-derived trophic factors transiently enhanced electrical synaptic connectivity and suppressed calcium-dependent exocytosis. Fluorescence imaging demonstrated that cells, with or without trophic factor treatment, were capable of producing similar elevations in presynaptic calcium. Therefore, differences in ability to buffer presynaptic calcium were not the basis for differential synaptic responses between groups. Unlike other systems where calcium has been reported to permeate gap junctions in electrotonically coupled cells (Saez et al., 1989; Christ et al., 1992), detectable levels of calcium did not pass between tightly coupled B110-B19 neuronal pairs. Therefore, gap junctional conduits connecting these synaptic partners were not a source of significant shunting of calcium following presynaptic accumulation. Consequently, the transient development of electrical synapses disrupted a process downstream of the calcium accumulation mediating vesicular release of neurotransmitter.

Since intracellular calcium concentration changes were similar in the presence and absence of trophic factor-induced electrical coupling, mechanisms downstream, linking calcium with vesicular release, must have been responsible for differences in chemical synaptic connectivity. Vesicle mobilization in CM pairs appeared normal, or possibly enhanced, despite the fact that transmitter release was compromised during electrical synaptogenesis. Therefore, we conclude that electrical synapses do not disrupt the developmental recruitment of a presynaptic pool of vesicles; however, this pool is not readily releasable. An essential component of chemical neurotransmission is the movement of vesicles from the reserve pool to the readily releasable vesicles (Kuromi and Kidokoro, 2003). Once mobilized, vesicular release occurs randomly throughout the readily releasable pool, possibly due to the ease of vesicle detachment from cytoskeletal elements (Rizzoli and Betz, 2004). Since gap junctional proteins form complexes with nearby cytoskeletal proteins (Toyofuku et al., 1998; Rash et al., 2004), the possibility exists that a direct interaction could occur between gap junctional proteins and synaptic vesicle proteins, thus altering the availability of vesicles for release.

Alternatively, transient electrical synapses could perturb local cellular signaling by altering the levels of presynaptic second messengers or the local cellular events they mediate. Chemical neurotransmission depends on a conglomerate of cytosolic, vesicle-associated, and plasma membrane-bound proteins. Interaction between these proteins is highly dependent on phosphorylation states (Fujita et al., 1996). For example, synapsins regulate vesicle mobilization by linking the synaptic vesicles to actin utilizing a phosphorylation-dependent mechanism (Pieribone et al., 1995). In addition, many regulators of SNARE (soluble *N*-ethymaleimide-sensitive fusion protein attachment protein receptors) proteins and vesicle fusion, such as Sec1/Munc18, synaptotagmin, and tomosyn, are phosphorylated during the regulation of SNARE function (Gerst, 2003). Therefore, critical elements of the

secretion machinery are susceptible to altered function due to gap junctional influences on intracellular signaling.

Gap junction formation varies depending on cell type, but electrical synapses generally arise from the insertion of hemichannels into the plasma membrane, and subsequently form plaques as junctional proteins accumulate at the periphery of developing clusters of connexons (Johnson et al., 2002; Gaietta et al., 2002; Lauf et al., 2002). A potential explanation for an inverse relationship between electrical and chemical neurotransmission might involve the physical disruption of the active zone machinery by this process of plaque formation. That is, the spatial requirements of gap junctional plaques might exclude the function or construction of the components necessary for chemical transmission, consequently impeding vesicle exocytosis. Since mixed synapses exist in some systems where both electrical and chemical neurotransmission function in close proximity (Lin and Faber, 1988; Rash et al., 1996), gap junctional obstruction of synaptic vesicle release is not likely, but nevertheless a possibility.

The enhancement of electrical transmission, and subsequent reduction in chemical neurotransmission, was accomplished by the exposure of neurons to trophic factors released into the culture medium from damaged neural tissue (Wong et al., 1981; Barker et al., 1982). Some of these ganglia-derived factors have been identified and shown to individually alter synapse formation (Magoski and Bulloch, 1998; Munno et al., 2000). One potential target of this modulation is calcium signaling, since voltage-gated ion channels are affected by trophic factors (Lesser et al., 1999; Yamuy et al., 2000). In this study, the increase in transient electrical coupling and the reduction in neurotransmitter release were not due to changes in voltage-gated currents, since the disruption occurred downstream of calcium influx.

Besides promoting cell survival (Oppenheim et al., 1992; Pinzon-Duarte et al., 2004) and neuronal differentiation (McAllister et al., 1997; Cohen-Cory, 1999; Lom and Cohen-Cory, 1999), trophic factors regulate several aspects of synaptic transmission (Lohof et al., 1993; Kang and Schuman, 1995; Boulanger and Poo, 1999) and alter electrical communication between neurons (Nadarajah et al., 1998; Reuss et al., 1998; Aberg et al., 2000; Szabo et al., 2004). Furthermore, knockouts of both trophic factors (Martinez et al., 1999) and their receptors (Pozzo-Miller et al., 1999) contain decreased levels of presynaptic vesicle density. For these reasons, the temporal appearance of trophic factors during development profoundly impacts neural network formation. During the initial phases of synaptogenesis, the synchrony of neuronal activities can be electrotonically governed (Kandler and Katz, 1995). Transient electrical coupling has been detected in many systems prior to the emergence of chemical connectivity at developing and regenerating synapses, thus regulation of gap junctional communication by trophic factors serve as a functional switch between two forms of synaptic transmission: chemical and electrical. In regenerating *Helisoma* neurons, the duration that electrotonic coupling coincides with the length of time that is required for extending axons to establish growth cone contacts with potential targets. The decline of neural network coupling following the downregulation of electrical synaptic transmission is replaced by inhibitory chemical synaptogenesis within the nervous system (Szabo et al., 2004). The question remains to be determined as to whether or not this functional shift in synaptic communication is regulated by trophic factor signaling in vivo. Nevertheless, the mechanism by which electrical connections (or simultaneous mechanisms induced by trophic factors) disrupt neurotransmission is downstream of both calcium influx and vesicle mobilization. Since these *Helisoma* neurons possess the ability to release neurotransmitter following several days of trophic factor exposure, but lose this capacity as electrical synapses form (Szabo et al., 2004), it is unlikely that trophic factors alone cause this reduction in chemical synaptic transmission. Thus, transient electrical synapse formation, alone or in conjunction with other trophic factor-induced mechanisms, likely inhibits synaptic vesicles from acquiring a readily releasable state. It will be important to determine whether the expression of gap junctions at developing synaptic contacts impart this negative influence on the exocytotic process and what molecular components of the secretory apparatus might be impacted.

ACKNOWLEDGMENTS

We thank Drs. Theresa Szabo and Robert Burghardt for comments on the manuscript and technical advice. Image analysis was conducted in the Cellular Physiology and Molecular Imaging Laboratory at Texas A&M University.

REFERENCES

Aberg ND, Carlsson B, Rosengren L, Oscarsson J, Isaksson OG, Ronnback L, Eriksson PS. 2000. Growth hormone increases connexin-43 expression in the cerebral cortex and hypothalamus. Endocrinology 141:3879–3886.

Allen F, Warner A. 1991. Gap junctional communication during neuromuscular junction formation. Neuron 6:101–111.

Barker DL, Wong RG, Kater SB. 1982. Separate factors produced by the CNS of the snail *Helisoma* stimulate neurite outgrowth and choline metabolism in cultured neurons. J Neurosci Res 8:419–432.

Bennett MV, Zukin RS. 2004. Electrical coupling and neuronal synchronization in the Mammalian brain. Neuron 41:495–511.

Bittman K, Owens DF, Kriegstein AR, LoTurco JJ. 1997. Cell coupling and uncoupling in the ventricular zone of developing neocortex. J Neurosci 17:7037–7044.

Boulanger LPoo MM. 1999. Gating of BDNF-induced synaptic potentiation by cAMP. Science 284:1982–1984.

Bulloch AG, Kater SB. 1981. Selection of a novel connection by adult molluscan neurons. Science 212:79–81.

Bulloch AG, Kater SB, Murphy AD. 1980. Connectivity changes in an isolated molluscan ganglion during in vivo culture. J Neurobiol 11:531–546.

Chang Q, Pereda A, Pinter MJ, Balice-Gordon RJ. 2000. Nerve injury induces gap junctional coupling among axotomized adult motor neurons. J Neurosci 20:674–684.

Cohen-Cory S. 1999. BDNF modulates, but does not mediate, activity-dependent branching and remodeling of optic axon arbors in vivo. J Neurosci 19:9996–10003.

Christ GJ, Moreno AP, Melman A, Spray DC. 1992. Gap junction-mediated intercellular diffusion of Ca2+ in cultured human corporal smooth muscle cells. Am J Physiol 263:C373–C383.

Curtin KD, Zhang Z, Wyman RJ. 2002. Gap junction proteins expressed during development are required for adult neural function in the *Drosophila* optic lamina. J Neurosci 22:7088–7096.

Fujita Y, Sasaki T, Fukui K, Kotani H, Kimura T, Hata Y, Sudhof TC, Scheller RH, Takai Y. 1996. Phosphorylation of Munc-18/n-Sec1/rbSec1 by protein kinase C: its implication in regulating the interaction of Munc-18/n-Sec1/rbSec1 with syntaxin. J Biol Chem 271:7265–7268.

Gaietta G, Deerinck TJ, Adams SR, Bouwer J, Tour O, Laird DW, Sosinsky GE, Tsien RY, Ellisman MH. 2002. Multicolor and electron microscopic imaging of connexin trafficking. Science 296: 503–507.

Gerst J. 2003. SNARE regulators: matchmakers and matchbreakers. Biochim Biophys Acta 1641:99–110.

Hadley RD, Wong RG, Kater SB, Barker DL, Bulloch AG. 1982. Formation of novel central and peripheral connections between molluscan central neurons in organ cultured ganglia. J Neurobiol 13: 217–230.

Hadley RD, Kater SB, Cohan CS. 1983. Electrical synapse formation depends on interaction of mutually growing neurites. Science 221: 466–468.

Hadley RD, Bodnar DA, Kater SB. 1985. Formation of electrical synapses between isolated, cultured *Helisoma* neurons requires mutual neurite elongation. J Neurosci 5:3145–3153.

Hamakawa T, Woodin MA, Bjorgum MC, Painter SD, Takasaki M, Lukowiak K, Nagle GT, Syed NI. 1999. Excitatory synaptogenesis between identified *Lymnaea* neurons requires extrinsic trophic factors and is mediated by receptor tyrosine kinases. J Neurosci 19:9306–9312.

Haydon PG, Kater, SB. 1988. The differential regulation of formation of chemical and electrical connections in *Helisoma.* J Neurobiol 19:636–655.

Haydon PG, Zoran MJ. 1989. Formation and modulation of chemical connections: evoked acetylcholine release from growth cones and neurites of specific identified neurons. Neuron 2:1483–1590.

Johnson RG, Meyer RA, Li XR, Preuss DM, Tan L, Grunenwald H, Paulson AF, Laird DW, Sheridan JD. 2002. Gap junctions assemble in the presence of cytoskeletal inhibitors, but enhanced assembly requires microtubules. Exp Cell Res275:67–80.

Kandler K, Katz LC. 1995. Neuronal coupling and uncoupling in the developing nervous system. Curr Opin Neurobiol 5:98–105.

Kandler K, Katz LC. 1998. Coordination of neuronal activity in developing visual cortex by gap junction-mediated biochemical communication. J Neurosci 18:1419–1427.

Kang HJ, Schuman EM. 1995. Neurotrophin-induced modulation of synaptic transmission in the adult hippocampus. J Physiol Paris 89:11–22.

Kuromi H, Kidokoro Y. 2003. Two synaptic vesicle pools, vesicle recruitment and replenishment of pools at the *Drosophila* neuromuscular junction. J Neurocytol 32:551–565.

Lauf U, Giepmans BN, Lopez P, Braconnot S, Chen SC, Falk MM. 2002. Dynamic trafficking and delivery of connexons to the plasma membrane and accretion to gap junctions in living cells. Proc Natl Acad Sci U S A 99:10446–10451.

Lesser SS, Holmes TM, Pittman AJ, Lo DC. 1999. Induction of electrical excitability by NGF requires autocrine action of a CNTF-like factor. Mol Cell Neurosci 14:169–179.

Lin JW, Faber F. 1988. Synaptic transmission mediated by single club endings on the goldfish Mauthner cell. I. Characteristics of electrotonic and chemical postsynaptic potentials. J Neurosci 8: 1302–1312.

Lohof AM, Ip NY, Poo MM. 1993. Potentiation of developing neuromuscular synapses by the neurotrophins NT-3 and BDNF. Nature 363:350–353.

Lom B, Cohen-Cory S. 1999. Brain-derived neurotrophic factor differentially regulates retinal ganglion cell dendritic and axonal arborization in vivo. J Neurosci 19:9928–9938.

Magoski NS, Bulloch AGM. 1998. Trophic and contact conditions modulate synapse formation between identified neurons. J Neurophysiol 79:3279–3283.

Martinez A, Alcantara S, Borrell V, Del Rio JA, Blasi J, Otal R, Campos N, Boronat A, Barbacid M, Silos-Santiago I, Soriano E. 1999. TrkB and TrkC signaling are required for maturation and synaptogenesis of hippocampal connections. J Neurosci 18:7336–7350.

McAllister AK, Katz LC, Lo DC. 1997. Opposing roles for endogenous BDNF and NT-3 in regulating cortical dendritic growth. Neuron 18:767–778.

Mentis GZ, Diaz E, Moran LB, Navarrete R. 2002. Increased incidence of gap junctional coupling between spinal motoneurones following transient blockade of NMDA receptors in neonatal rats. J Physiol 544:757–764.

Munno DW, Woodin MA, Lukowiak K, Syed NI, Dickinson PS. 2000. Different extrinsic trophic factors regulate neurite outgrowth and synapse formation between identified Lymnaea neurons. J Neurobiol 44:20–30.

Murphy AD. 2001. The neuronal basis of feeding in the snail, Helisoma, with comparisons to selected gastropods. Prog Neurobiol 63:383–408.

Nadarajah B, Makarenkova H, Becker DL, Evans WH, Parnavelas JG. 1998. Basic FGF increases communication between cells of the developing neocortex. J Neurosci 18:7881–7890.

Nicholson SM, Bruzzone R. 1997. Gap junctions: getting the message through. Curr Biol 7:340–344.

Oppenheim RW, Yin QW, Prevette D, Yan Q. 1992. Brain-derived neurotrophic factor rescues developing avian motoneurons from cell death. Nature 360:755–757.

Pastor AM, Mentis GZ, De La Cruz RR, Diaz E, Navarrete R. 2003. Increased electrotonic coupling in spinal motoneurons after transient botulinum neurotoxin paralysis in the neonatal rat. J Neurophysiol 89:793–805.

Penn AA, Wong RO, Shatz CJ. 1994. Neuronal coupling in the developing mammalian retina. J Neurosci 14:3805–3815.

Personius K, Chang Q, Bittman K, Panzer J, Balice-Gordon R. 2001. Gap junctional communication among motor and other neurons shapes patterns of neural activity and synaptic connectivity during development. Cell Commun Adhes 8:329–333.

Pieribone VA, Shupliakov O, Brodin L, Hilfiker-Rothenfluh S, Czernik AJ, Greengard P. 1995. Distinct pools of synaptic vesicles in neurotransmitter release. Nature 375:493–497.

Pinzon-Duarte G, Arango-Gonzalez B, Guenther E, Kohler K. 2004. Effects of brain-derived neurotrophic factor on cell survival, differentiation and patterning of neuronal connections and Muller glia cells in the developing retina. Eur J Neurosci 19: 1475–1484.

Poyer JC, Zoran MJ. 1996. Activity-dependent induction of functional secretory properties at cultured neuromuscular synapses of *Helisoma*. J Neurophysiol 76:2635–2643.

Pozzo-Miller LD, Gottschalk W, Zhang L, McDermott K, Du J, Gopalakrishnan R, Oho C, Sheng ZH, Lu B. 1999. Impairments in high-frequency transmission, synaptic vesicle docking, and synaptic protein distribution in the hippocampus of BDNF knockout mice. J Neurosci 19:4972–4983.

Rash JE, Dillman RK, Bilhartz BL, Duffy HS, Whalen LR, Yasumura T. 1996. Mixed synapses discovered and mapped throughout mammalian spinal cord. Proc Natl Acad Sci U S A 93:4235–4239.

Rash JE, Pereda A, Kamasawa N, Furman CS, Yasumura T, Davidson KG, Dudek FE, Olson C, Li X, Nagy JI. 2004. High-resolution proteomic mapping in the vertebrate central nervous system: close proximity of connexin35 to NMDA glutamate receptor clusters and co-localization of connexin36 with immunoreactivity for zonula occludens protein-1 (ZO-1). J Neurocytol 33:131–151.

Reuss B, Dermietzel R, Unsicker K. 1998. Fibroblast growth factor 2 (FGF-2) differentially regulates connexin (cx) 43 expression and function in astroglial cells from distinct brain regions. Glia 22:19–30.

Rizzoli SO, Betz WJ. 2004. The structural organization of the readily releasable pool of synaptic vesicles. Science 303:2037–2039.

Saez JC, Connor JA, Spray DC, Bennett MV. 1989. Hepatocyte gap junctions are permeable to the second messenger, inositol 1,4,5-trisphosphate, and to calcium ions. Proc Natl Acad Sci U S A 86: 2708–2712.

Spitzer NC. 1982. Voltage- and stage-dependent uncoupling of Rohon-Beard neurones during embryonic development of *Xenopus* tadpoles. J Physiol 330:145–162.

Sutor B. 2002. Gap junctions and their implications for neurogenesis and maturation of synaptic circuitry in the developing neocortex. Results Probl Cell Differ 39:53–73.

Szabo TM, Faber DS, Zoran MJ. 2004. Transient electrical coupling delays the onset of chemical neurotransmission at developing synapses. J Neurosci 24:112–120.

Toyofuku T, Yabuki M, Otsu K, Kuzuya T, Hori M, Tada M. 1998. Direct association of the gap junction protein connexin-43 with ZO-1 in cardiac myocytes. J Biol Chem 273:12725–12731.

Veenstra RD, Wang HZ, Beblo DA, Chlton MG, Harris AL, Beyer EC, Brink PR. 1995. Selectivity of connexin-specific gap junctions does not correlate with channel conductance. Circ Res 77:1156–1165.

Wong RG, Hadley RD, Kater SB, Hauser GC. 1981. Neurite outgrowth in molluscan organ and cell cultures: the role of conditioning factor(s). J Neurosci 1:1008–1021.

Yamuy J, Pose I, Pedroarena C, Morales FR, Chase MH. 2000. Neurotrophin-induced rapid enhancement of membrane potential oscillations in mesencephalic trigeminal neurons. Neuroscience 95:1089–1100.

Zoran MJ, Doyle RT, Haydon PG. 1991. Target contact regulates the calcium responsiveness of the secretory machinery during synaptogenesis. Neuron 6:145–151.

Zoran MJ, Metts BA, Poyer JC. 1996. Specific muscle contacts induce increased transmitter release and neuritic arborization in motoneuronal cultures. Dev Biol 179:212–222.